Title

Nature of Zirconia on a Copper Inverse Catalyst Under CO2 Hydrogenation Conditions

Journal

Journal of the American Chemical Society, 145(48)

ISSN

0002-7863

Authors

Kumari, Simran
Alexandrova, Anastassia N
Sautet, Philippe

Publication Date

2023-12-06

DOI

10.1021/jacs.3c09947

Nature of Zirconia on Copper Inverse Catalyst under CO_2 Hydrogenation Conditions

Simran Kumari[a], Anastassia N. Alexandrova[b,c,t,*], Philippe Sautet[a,b,d,k,*]

[a] Department of Chemical and Biomolecular Engineering, University of California, Los Angeles, CA 90095, United States

[b] Department of Chemistry and Biochemistry, University of California, Los Angeles, CA 90095, United States

[c]Department of Materials Science and Engineering, University of California, Los Angeles, CA 90095, United States

[d]California NanoSystems Institute, University of California, Los Angeles, CA 90094, United States

[t]ana@chem.ucla.edu, [k]sautet@ucla.edu

[*]Corresponding Author

ABSTRACT

The growing concern over the escalating levels of anthropogenic CO_2 emissions necessitates effective strategies for its conversion into valuable chemicals and fuels. In this research, we embark on a comprehensive investigation of the nature of the zirconia on copper inverse catalyst under the conditions of CO_2 hydrogenation to methanol. We employ density functional theory calculations in combination with the Grand Canonical Basin Hopping method, enabling an exploration of the free energy surface including a variable amount of adsorbates within the relevant reaction conditions. Our focus centers on a model three atom Zr cluster on a Cu(111) surface decorated with various O, OH and formate ligands, noted $Zr_3O_x(OH)_y(HCOO)_z$/Cu111, revealing major changes in the active site induced by various reaction parameters such as the gas pressure, temperature, conversion levels, and CO_2:H_2 feed ratios. Through our analysis, we have unveiled insights into the dynamic behavior of the catalyst. Specifically, under reaction conditions, we observe a large number of composition and structures with similar free energy for the catalyst, with respect to changing the type, number, and binding sites of adsorbates, suggesting that the active site should be regarded as a statistical ensemble of diverse structures that easily interconvert.

I. INTRODUCTION

By 2050, the amount of human-produced CO_2 is expected to rise significantly. The burning of fossil fuels, which emits CO_2 into the atmosphere, is primarily to blame for this increase. Being one of the main greenhouse gases causing climate change and global warming, the growing concentration of CO_2 is a serious concern. However, CO_2 may also be seen as an alternative feedstock, and recycling it into value-added chemicals can produce a fuel cycle that is carbon neutral. The process of CO_2 hydrogenation, which turns CO_2 into methanol using hydrogen, is one possible method of CO_2 recycling [1–12]. Methanol is a liquid fuel that may be used as a substitute for gasoline in the transportation sector.[13] Furthermore, using the methanol-to-olefins (MTO) method, methanol may be directly transformed into useful compounds such as ethylene, and utilized as a raw material for synthesizing higher hydrocarbons and oxygenates.

Copper-based catalysts have become the standard choice for methanol synthesis [14–16]. In particular, the commercial $Cu/ZnO/Al_2O_3$ catalyst has been widely used to convert synthesis gas, which is a mixture of CO, hydrogen, and some CO_2, into methanol at the temperatures range of 220-300 °C and pressures of 50-100 bar [6,17,18] . Significant efforts have been devoted to improving the catalytic performance of the Cu-based catalysts. An enhancement in CO_2/H_2 conversion and CH_3OH selectivity was achieved by forming Cu alloys[19,20], and using metal oxides as supports for Cu. Among the Cu on oxide catalysts studied, zirconia-modified copper catalysts have been shown to be effective in CO_2/H_2 conversion to methanol due to their high stability under reducing or oxidizing conditions [15,21–35]. Denise et al.[36] discovered that under 1 bar pressure, Cu/ ZrO_2 with a low Cu loading (1-2 wt %) demonstrates methanol yields comparable to those of commercial $Cu/ZnO/Al_2O_3$ (45-50 wt % Cu) catalysts during CO_2 hydrogenation. They suggest that the ZrO_2 support should be regarded as an essential component of the "active site" due to its influential role in the hydrogenation mechanism, enabling to suppress CO and methane byproducts[34]. Larmier et al. (2017) found that ZrO_2 enhances both the methanol production rate and the selectivity[38] of methanol vs methane compared to other copper-based catalysts. Samson et al. (2014) studied Cu/ ZrO_2 catalysts obtained by impregnation of ZrO_2 and complexation with citric acid for CO_2 hydrogenation to methanol[33]. In recent works, inverse ZrO_2 on Cu (ZrO_2/Cu) catalysts have also gained a lot of traction as they display high activity, selectivity, and stability during the conversion of CO_2 to methanol. Rodriguez and coll. (2021) investigated the CO_2 hydrogenation on ZrO_2/Cu (111) inverse model catalysts and found these to

display high stability and activity for the hydrogenation of CO_2 into methanol at 500-600 K[21] . Notably, their findings revealed that the catalyst composed of only 10% ZrO_2 on Cu demonstrated three times greater activity when compared to a conventional zirconia-supported Cu catalyst. Wu et al. (2020) reported that inverse ZrO_2/Cu catalysts with a tunable Zr/Cu ratio have been prepared via an oxalate co-precipitation method, showing excellent performance for CO_2 hydrogenation to methanol[26]. The study found that most of the ZrO_2 particles had a size around 1.2 nm and that even a very small amount of Zr (10%) on Cu(90%) is highly active for CO_2 hydrogenation to methanol. White and coll. also studied CO_2 hydrogenation for the model inverse Zr/Cu_2O/Cu(111) catalyst and found the promotional effects of small amorphous zirconia particles for increasing CO_2 adsorption and the formation of hydrogenated intermediates on the CuO_2/Cu(111) surface[39]. A fundamental understanding of the nature and structure of surface active sites on the inverse catalyst, ZrO_2 supported on Cu, is hence of great importance.

Numerous studies have been conducted to explore the adsorbates that accumulate on catalyst surfaces under reaction conditions. This line of research is crucial as these adsorbates can significantly alter the size and shape of the catalytic particles or clusters [40–46]. In the case of CO_2 hydrogenation, hydroxyls and formates are commonly identified as the primary ligands that accumulate on the catalyst surface, with certain formates undergoing further hydrogenation to produce methoxy and methanol. However, the quantity and diversity of adsorbates on the surface can vary considerably depending on the specific reaction conditions. For instance, White and coll. observed at low pressure (0.013atm) that formates, methoxy, and hydroxyls were the main species present on the model inverse catalyst. However, the amount of formate was relatively low compared to other ligands such as methoxy, and the number of hydroxyls decreased with increasing temperature[39]. In contrast, Rodriguez and coll. reported at higher pressure (4.93atm) the presence of a high amount of formate and methoxy species on the ZrO_2 supported on Cu catalyst. Interestingly, the formates present on the ZrO_2 cluster showed low reactivity and remained inactive during the reaction, while the formates at the interface exhibited high activity. This was determined by analyzing the changes in operando DRIFTS intensity generated by formates at the interface and formates on the cluster during the reaction condition. The intensity of the formates at the interface decreased significantly after a reaction time of more than 90 minutes, whereas the formates on the cluster did not show significant changes. These studies

underscore the significance of considering the structure of the catalytic cluster when exposed to different ligands (-O, -OH, -HCOO) in reaction conditions. Such an understanding is essential for elucidating the active site and the mechanism of CO_2 hydrogenation on these catalysts.

In our current study, we are primarily focused on identifying a collection of low energy structures that could potentially contain the combined active site responsible for CO_2 hydrogenation. This is heavily influenced by the reaction conditions, that control the type and number of adsorbates present on the cluster. Furthermore, we investigate the electronic state of the catalyst to explore the synergy between Zr and Cu at the interface and their potential role in facilitating CO_2 adsorption and hydrogenation.

In this manuscript, we first examine how different reaction conditions impact the free energy surface of the catalyst in the presence of ligands, via detailed sampling of multi-adsorbates configurations using first principle grand canonical basin hopping simulations (GCBH) .The GCBH tool is crucial for a detailed sampling the configurations of catalysts' surfaces in given pressure and temperature condition, studying the dynamic behavior of catalysts and providing insights into the diverse active phases that adjust to specific reaction conditions, thus aiding in the rational design of efficient catalysts. Using these tools, we show that the catalyst has an extremely flat free energy surface with respect to the changes of the type, number, and binding sites of adsorbates, meaning that several possible structures have similar free energies and thus co-exist in reaction conditions, collectively constituting the ensemble of active sites. Subsequently, we elucidate the effect of specific cases of reaction conditions on the catalyst. We find that different experimental conditions reported in the literature in fact correspond to different ensembles of the catalyst states, suggesting that the mechanistic differences observed in different works may have an underlying cause due to catalyst itself changing. Finally, we discuss the electronic properties of the catalyst and provide insight relevant to potential mechanisms of CO_2 hydrogenation.

II. COMPUTATIONAL MODEL AND METHODS

1. *Model:* The Cu(111) surface with a small adsorbed Zr cluster consisting of three Zr atoms were selected as the model for studying the catalytic properties of the zirconia-copper inverse catalyst for CO_2 hydrogenation. The Cu(111) surface is a commonly used model

for studying the catalytic properties of copper-based catalysts due to its high stability and well-defined surface structure. The small zirconia cluster containing three Zr atoms was chosen to maintain the computational cost reasonable while still accurately representing the active sites of the zirconia-copper inverse catalyst. Experiments have shown that bulk ZrO_2 is not required in the catalysts, and that highly dispersed species can be highly active[25]. Three Zr atoms on a 5x5 Cu(111) unit cell also represents a 12% coverage of Zr, which was found to be the optimum coverage for the highest CH_3OH conversion and selectivity[26]. 20 Å of vacuum was added between the slabs. Using this model, the optimum coverage of oxygen, hydroxyl, and formate species on the zirconia-copper inverse catalyst under CO_2 hydrogenation conditions was investigated. The goal was to identify the most stable and the low energy metastable configurations for these adsorbates on the model catalyst surface, which could provide valuable insights into the catalytic activity of the material.

2. *Total Energy Calculations:* All calculations were carried out within the density functional theory framework using the Vienna ab-initio simulation package (VASP)[47,48]. The electron-ion interactions were treated using the projector augmented wave (PAW) method[49]. We used the Perdew–Burke–Ernzerhof (PBE) functional to calculate the exchange-correlation energy[50]. The Gaussian method with a smearing of 0.1eV was used to improve the k-point convergence. The valence electronic states were expanded in a plane-wave basis set with an energy cutoff of 400 eV. A 5x5 supercell of Cu(111) was selected (lattice constant: 12.76 Å) and the Brillouin-zone (BZ) integration was sampled by adopting the Monkhorst–Pack (MP) k-point grids of 3x3x1 for all the surfaces. During the geometry relaxations of the surface, only the outer atoms were allowed to relax. The cell parameters and the bottom two of the total five layers of Cu were fixed to those determined for bulk Cu. Dipole corrections were included to correct for spurious dipolar interactiosn between slabs. Structures were relaxed until the force on each atom was less than 0.01 eV/ $Å^{-1}$.

3. *Grand Canonical Basin Hopping:* To investigate the possible adsorption sites of the cluster on the Cu surface, the cluster shape, and the optimum number and placement of adsorbates on the zirconia-copper inverse catalyst under CO_2 hydrogenation conditions,

we employed the Grand Canonical Basin Hopping (GCBH) method, the full detail of the algorithm is given in supplementary information (SI 1). The sampling moves and settings within GCBH were as follows:

1. The Zr atoms were allowed to move freely on the surface, enabling them to find various modes of adsorption and reconfigure the cluster core.
2. Oxygens and hydroxyls were added grand canonically in the GCBH process, subject to the chemical potential change defined by the experimental conditions. The Oxygens and hydroxyls can also change positions around the cluster and can spill over on the Cu surface.
3. The adsorption site and geometry of the overall cluster could also be altered by the oxygens and hydroxyls.
4. The formates were added one at a time, up to a maximum of four formates, and we explored the free energy surface for each number of formate adsorbates. Formates could adsorb, desorb, change the adsorption sites for O and OH species, and change the geometry of the Zr cluster and their binding mode: at the Zr/Cu interface, on the Cu surface, at the bridging position between two Zr atoms, or on just one Zr atom.

4. *Chemical potential of adsorbates:* To accurately replicate the reaction conditions for the CO_2 hydrogenation reaction, it is essential to calculate the chemical potentials of all species involved. To define the reaction condition, four main parameters are considered: (a) total pressure, (b) the CO_2:H_2 ratio in the initial feed, (c) the temperature at which the reaction is conducted, and (d) the conversion of the reaction shown in the following equation, which provides the partial pressures of reactants and products:

$$CO_2 + 3H_2 \rightarrow HCOO + 2.5H_2 \rightarrow CH_3OH + H_2O$$

The chemical potential of O is calculated using the formula $\mu(O) = \mu(H_2O) - \mu(H_2)$. The chemical potential of OH is calculated using the formula $\mu(OH) = \mu(H_2O) - 0.5\mu(H_2)$, The chemical potential of HCOO is calculated using the formula $\mu(HCOO) = \mu(CO_2) + 0.5\mu(H_2)$, where $\mu(CO_2)$ is the chemical potential of CO_2. The chemical potentials of H_2 and H_2O are calculated in the vapor phase using the ideal gas approximation.

5. *Free energy*: The free energy of the adsorbed cluster with -O, -OH and -HCOO ligands reported throughout the work is evaluated via the following equation:

$$\Delta G = E\left(Zr_3O_xOH_y\,(HCOO)_z\,/Cu(111)\right) - E\left(Zr_3O_6\,/Cu(111)\right) - (x-6)\mu_O - y\mu_{OH} - z\mu_{HCOO}$$

Here the $Zr_3O_xOH_y\,(HCOO)_z\,/Cu(111)$ represents the energy of the $Zr_3O_xOH_y\,(HCOO)_z$ cluster supported on the Cu(111) surface. x, y, and z signify the number of O, OH, and formate adsorbates on the cluster, respectively. Additionally for convenience, we use as a reference the energy of $Zr_3O_6\,/Cu(111)$ in its global energy minimum state. We selected $Zr_3O_6\,/Cu(111)$ as our reference because it is one of the most used representative systems in the literature for studying CO_2 hydrogenation on inverse ZrO_2/Cu catalysts[34,51,52].

III. RESULTS AND DISCUSSION

A. Free energy surface of $Zr_3O_xOH_y\,(HCOO)_z\,/Cu(111)$ at different reaction condition

Our first objective was to determine the free energy surface of the $Zr_3O_xOH_y\,(HCOO)_z\,/Cu(111)$ system, using the GCBH method. Three different reaction conditions were chosen to represent a variety of literature experimental works, where P is the total pressure, T the temperature and C the conversion: (a) P = 0.013atm, T = 500K, CO_2/H_2 ratio = 9, and C = 2% corresponding to the work of White and coll. [39], (b) P = 4.93 atm, T = 493.15K, CO_2/H_2 ratio = 1:3, and C = 0.8% corresponding to the work of Liu and coll. [34], and (c) P = 30 atm, T = 493.15 K, CO_2/H_2 ratio = 3, and C = 19.4% (equilibrium conversion for CO_2 hydrogenation at the given conditions) corresponding to the work of Ma and coll. [26]. The results of the GCBH simulations are depicted in Fig 1(a), with the purple lines representing condition (a), the blue lines representing condition (b), and the green lines representing condition (c). The structures within the energy range of 0.75 eV from the global minima (GM) for each number of formates, ranging from 0 to 4, are shown in the plot. The bulk like composition Zr_3O_6/Cu(111) is never the most stable one, by at least ~1.5 eV. The energy landscape of the $Zr_3O_xOH_y\,(HCOO)_z\,/Cu(111)$ system exhibits significant changes under different reaction conditions, with a free energy minimum for zero formate at low pressure shifting to 2-4 formates at higher pressure. This shows that the reaction conditions play a crucial role in determining the most stable ensemble of configurations of the system. As the

initial feed pressure increases, the preferred HCOO/Zr ratio of the system also increases. However, this ratio also depends on the conversion. As we approach the equilibrium conversion of CO_2 hydrogenation (P = 30atm, temp = 493.15 K, CO_2/H_2 ratio = 3) , the formate/Zr ratio becomes 1:1. It is noteworthy that the stability of the various adsorbates (-O, -OH, -HCOO) on the $Zr_3O_xOH_y(HCOO)_z$ /Cu(111) model catalyst is not only influenced by the number and type of adsorbates on the cluster, but also by the reaction conditions. At a higher pressure of the initial feed, the overall stability of the adsorbates on the cluster in relation to the Zr_3O_6/Cu (111) system expectedly increases (corresponding to more negative free energies).

To further investigate the probability distribution of different configurations at respective reaction temperatures, we calculated the Boltzmann probability $P_I = \frac{1}{z}\exp\left[\frac{-\Delta G_I}{K_B T}\right]$, for each structure, where I represents the structure, marking the likelihood of its occurrence under specific reaction conditions. ΔG_I is referred to the putative global minimum and incorporates entropy contributions from the various adsorbate chemical potentials while excluding the vibrational entropy of the cluster in order to manage computational expenses. For case (a), we observe that the Boltzmann probability is accumulated on one structure (with 88% probability), and on one other minor configuration (5%). However, for case (b), the free energy surface is very flat around the 2, 3 and 4 formate structures, which leads to highly distributed Boltzmann probability across a large ensemble of structures. In the last case (c), we observe that the Boltzmann probability is again distributed on a large number of structures, containing 2 or 3 formates. In the following sections we inspect in more details the first two reaction conditions to understand the real nature of the catalyst in the reaction condition. These two conditions, (a) and (b), were chosen because they represent two contrasting cases in terms of pressure, CO_2/H_2 ratio, and conversion. By investigating both extremes, we gain a comprehensive understanding of the $Zr_3O_xOH_y(HCOO)_z$ / Cu (111) catalyst's behavior, stability, and reactivity across a range of realistic and non-standard conditions. This approach provides valuable insights into the catalyst's versatility and its potential application under various reaction conditions, which can be critical for designing efficient catalytic processes for CO_2 hydrogenation.

B. Reaction condition (a): P = 0.013atm, Conv. = 2%, T = 500K, CO_2/H_2 ratio: 1:9

Figure 2 displays the side and top views of the five most favorable structures obtained using GCBH under reaction condition (a). The energies relative to the ground state are provided below each structure. The bottom colored panel illustrates the Boltzmann distribution of all unique structures obtained. Each structure for the ZrO_2/Cu system in the top panel is framed by a color-coded border, matching the color scheme of the Boltzmann distribution in the lower panel. The free energy surface heat plot at different oxygen, hydroxyl and formate coverages are provided SI-2. The $Zr_3O_3(OH)_3$ configuration was found to be dominant, with a high 88% Boltzmann population. It was also observed that a smaller population for $Zr_3O_4(OH)_3$ was present (5 %). In the energetically most favorable structures, the hydroxyl groups in the cluster were found to preferentially interact with Zr and not with Cu atoms, forming Zr-OH bonds. The oxygen atoms in the cluster tend to form Zr-O-Zr bridging bonds, linking the Zr atoms together. As the number of oxygen atoms increases, as in the case of $Zr_3O_4(OH)_3$, the oxygen atoms also start interacting with the Cu(111) surface, acting as an anchor for the cluster on the surface.

Additionally, we observed a relatively small population of formate-containing clusters, such as $Zr_3O_3(OH)_2HCOO$, $Zr_3O_3(OH)_3HCOO$, and $Zr_3O_3(OH)_2(HCOO)_2$, the total Boltzmann population of all formate containing structures being 4.5%. The presence of formate-containing clusters is relevant as it has been suggested that formate is an intermediate in the conversion of CO_2 to methanol and can accumulate on the cluster[19,21–24,26,38,51,53] . Therefore, understanding the formation and stability of formate-containing clusters could provide further insight into the reaction mechanism. The formate group in the $Zr_3O_3(OH)_2HCOO$ cluster replaces one of the hydroxyl groups in the $Zr_3O_3(OH)_3$ cluster and attaches to the same Zr atom in a bidentate fashion. As the number of hydroxyl groups increases, as in the case of $Zr_3O_3(OH)_3HCOO$, the hydroxyl groups occupy the same sites as they do in $Zr_3O_3(OH)_3$, but the formate group binds in a bridging position between the two Zr atoms in a bidentate fashion.

Interestingly, White and Coll. [39] found that vibrational bands associated with formate were generally weak in the IRAS spectra (IRAS was performed on Zr/Cu_2O/Cu(111) after exposure to CO_2/H_2 mixture), and the peaks assigned to formate in the C 1s XPS spectra were also weak compared to other intermediates. These observations suggested that formate was not accumulating on the surface during the reaction. Our results agree with these findings, where the global minimum of the cluster composition was observed as $Zr_3O_3(OH)_3$, whereas the structures

with formates were found to be metastable with low energy, i.e. sparsely and transiently populated.

In the CO_2 hydrogenation process, the hydrogenation of formate is the rate-determining step. The ways to lower the barrier for this step are either to weaken the strength of the adsorption of formate on the catalyst surface, or to enhance the adsorption of the hydrogenated product H_2COO. In our current reaction conditions, we have observed that the adsorption of formate on the catalyst surface is not very strong, resulting in minute populations of formate-containing structures, which could imply that the formates are readily being converted to hydrogenated H_2COO species.

As part of our investigation of the $Zr_3O_x(OH)_y(HCOO)_z$/Cu(111) system, we also studied the impact of temperature on the hydroxyl content of the cluster presented in Figure 3. It is known that hydroxyls are often bound at the surface of zirconia clusters and their presence can arise from various sources, including H atom spillover from Cu and dissociation of water formed via surface reactions such as reverse water gas shift (RWGS). Our findings revealed that hydroxyls are indeed bound to the zirconium atoms of the cluster, and their concentration exhibits a significant decrease as the temperature is increased from 300K to 600K (Figure 3). This is an important finding as the coverage of hydroxyls on the surface is anticipated to have a substantial influence on the reaction mechanism. At lower temperatures, the hydroxyl coverages are high, which occupies all the sites, which then would make it exceedingly difficult to bind CO_2 and initiate the CO_2 hydrogenation process. It is important to mention that our calculations are consistent with the O 1s XPS spectra reported by White and coll. [39], which illustrate that the surface concentration of OH* drops rapidly above ~ 450 K. This decrease in surface hydroxyl content could have significant implications for the hydrogenation of intermediates bound to zirconia and might contribute to the accumulation of H_xCO* species at higher temperatures.

C. Reaction condition (b): P = 4.93 atm, Conv. = 0.8%, CO_2/H_2 ratio = 1:3, and T = 493K

Reaction condition (b) represents a more realistic case, at a higher reactant pressure but still a low conversion. In Figure 4, we show the 5 most stable structures in the top panel, and in the lower panel, we show the distribution of Boltzmann probability among the ensemble of structures. The free energy surface heat plot at different oxygen, hydroxyl and formate coverages are provided SI-3. We can clearly observe that the Boltzmann probability is distributed over a

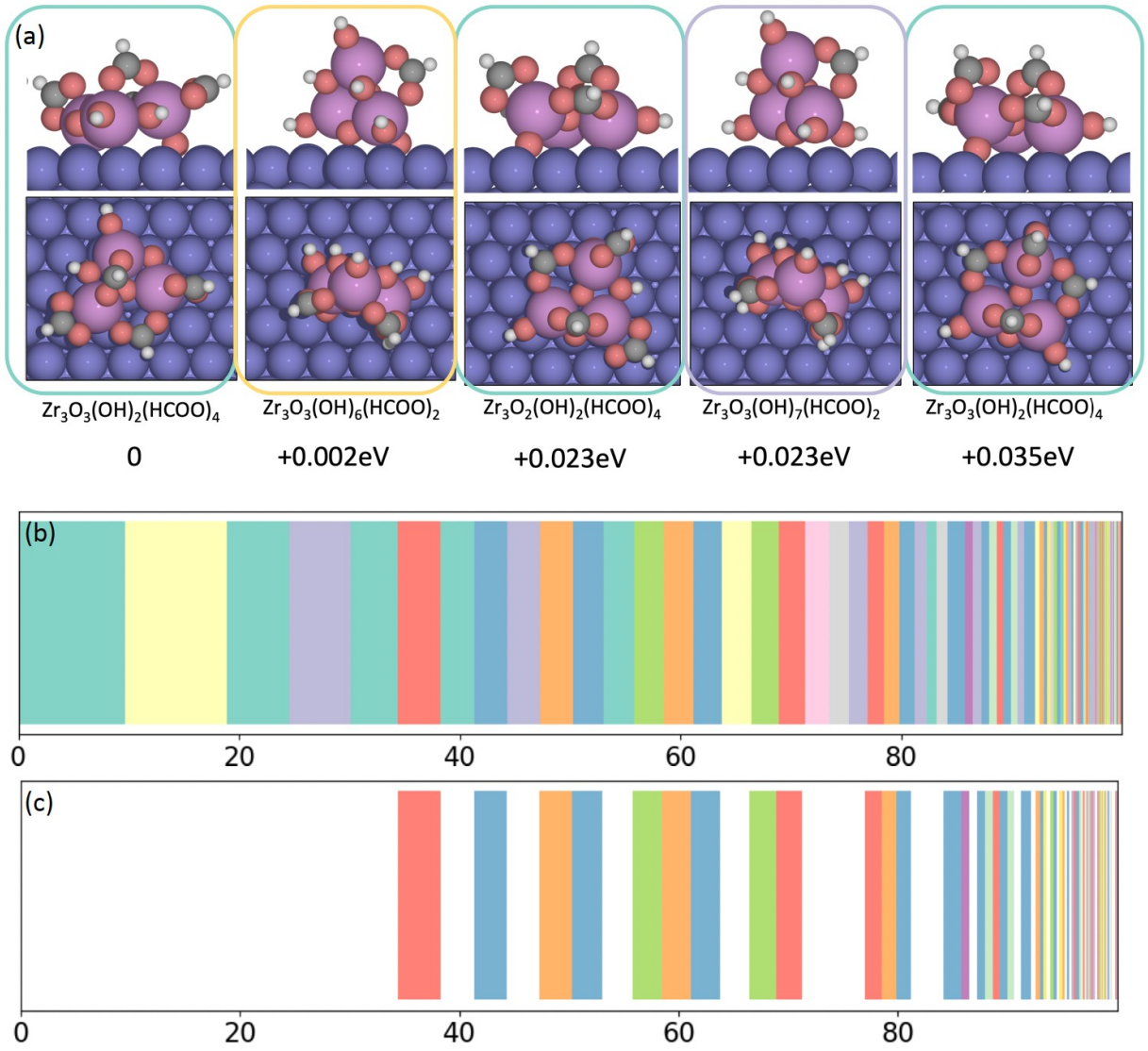

broad range of different cluster compositions and geometries. Compared to the low-pressure case (a), the key difference is that the population of formate-containing systems is very high (100% probability to find at least one formate), and the catalyst is covered by two to four formate molecules (see also Fig 1b). When considering the five best structures, which only represent 35% of the total population, we find that three out of the five structures have four formates on the cluster, while the other two have two formates on the cluster. The overall probability of finding 0, 1, 2, 3, and 4 formates on the cluster is 0, 0, 27.9, 41.8, and 30.4 % respectively. It can be underlined that structures with 3 formates appear as most probable, while none of the five most stable structures show 3 formates as represented in Fig 4 c. This underlines once the again the importance of considering the whole ensemble as accessible structures. Moreover, the number of

hydroxyls present in the cluster varies significantly across the structures, but that does not cause considerable energy changes. This observation suggests that the potential energy surface is very flat relative to the number of hydroxyls and formates present in the cluster. Therefore, the cluster can serve as a reservoir of hydroxyls and formates that can be utilized in subsequent steps of the reaction mechanism.

To understand the relative free energy between the ensemble of structures containing 0,1,2,3, and 4 formates, it could be important to calculate the "ensemble" statistical entropic contribution to the free energy of the system for the configuration corresponding to given number of formates. A statistical definition of entropy utilizing the Boltzmann probabilities of these discrete states was applied to obtain the "ensemble" statistical entropy $S_G = k_B \sum_I \square P_I \ln (P_I)$, where $P_I = \frac{e^{-G_I/k_B T}}{\sum e^{-G_I/k_B T}}$, the summation is running on the ensemble of structures (I) containing the specific number of formates, G_I is calculated as described in Section II.4 and incorporates contributions from E and Δμ, $\square_\square$ is the Boltzmann constant and T is the temperature. We can then include the "ensemble" statistical entropy to calculate the total G of the system as: $G_{tot} = G - TS_G$. Here, G represents the energy associated with the global minimum for the specific number of formates. This method has been utilized in other works: Alexandrova and coll. used it to describe the free energy of clusters with different ratios of Pt:Pd[54], and Manoharan et al used it to determine the free energy landscape of clusters[55]. Using this method, we provide the thermodynamic stability between the different number of formates in Figure 5. We can observe that the free energies start to stabilize as we reach the structures with 2HCOO, 3HCOO and 4HCOO with a minimum at 3HCOO. Therefore, as an ensemble, the 3 formate structures represent the free energy minimum. This is however similar to the result previously obtained in the absence of the ensemble entropy contribution, with the highest level of probability observed for 3HCOO at 41.8%.

In order to gain a more comprehensive understanding of the distribution of formate, OH, and O species on the cluster, we have plotted their probability distribution in Figure 6. The size of the circles in the plot corresponds to the prevalence of a specific configuration (one value of x, y and z) in the FES (i.e., a large circle corresponds to a high Boltzmann probability for the

given configuration). The darker shades indicate that a larger number of structures is associated with that set of adsorbate number. The total probability value for a given number of formates, where all number and structures for other adsorbates are included, is also given in the green box on the y axis of Figure 6a. Similarly, the total probability value for a given number of hydroxyls, or oxygens adsorbates is provide on the respective axis. The analysis reveals that the probability distribution is spread across various configurations, particularly between 2-4 formates, 2-7 hydroxyls, and 2-4 oxygens on the cluster. The probability range spans from 0% to 9.5%. This indicates that in the present reaction condition, no single state exhibits a clear dominance, in contrast to our observations in the previous section (case a). Instead, we observe a statistical ensemble of multiple states, which more accurately represents the catalytic site under catalytic conditions. It is important to note that the global minimum structure, i.e. the most stable configuration, may not even be the most mechanistically consequential. Therefore, when studying the CO_2 reaction mechanism, it is crucial to consider the ensemble of present catalyst states.

The presence of a diverse ensemble of easily accessible structures within the system provides significant advantages in facilitating the reaction mechanism and the formation of hydrogenated intermediate products. This diversity enables adjustment of the hydrogen and formate content without incurring significant energy costs. The accumulation of formate species on the cluster is a commonly observed phenomenon in studies related to CO_2 hydrogenation. Prior research by Liu et al [34] has highlighted the high adsorption energy of formate on the cluster, as determined through DFT simulations. Experimental evidence obtained through in situ DRIFTS measurements further supports this observation. Consistent with these previous findings, our work confirms the high coverage of formate on the cluster. We also observe that the adsorption of formate on the cluster reaches an optimal coverage, where the adsorption energy of formate stabilizes (Figure 1(a), blue lines). Furthermore, the hydroxyls present on the cluster serve as a hydrogen reservoir, providing an additional source of hydrogen not only for the hydrogenation of formates but also for that of other intermediate species.

D. Formates at the zirconia/copper interface

Numerous studies have found that the zirconia/copper interface plays a crucial role in the CO_2 hydrogenation reaction by facilitating the conversion of formate intermediates to methanol. One such study was conducted by Coperet et al.[38], who utilized a combined experimental and computational approach with realistic models, including kinetics, *in situ* IR and NMR spectroscopies, and isotopic labeling strategies. This study demonstrated that the reaction takes place specifically at the interface between zirconia and copper particles and that the formate species present at the interface between the Zr and Cu are more reactive. Another study conducted by Rodriguez and coll.[26] utilized IR measurements and observed a peak at 1350 cm^{-1} which is attributed to the symmetric O-C-O vibration of the formate species bonded on Cu or the interface, species noted formate-Cu. This peak was found to be about 18 cm^{-1} lower than that for formate adsorbed on the ZrO_2 (bidentate formate). The authors also observed that the generation and consumption of formate-Cu were extremely fast under transient conditions compared with the formate species on zirconia. This indicated that highly reactive pathways exist at the interface on the inverse catalyst. The Cu sites at the zirconia/copper interface were proposed to serve as the adsorption site for the formate intermediate, facilitating its hydrogenation conversion to methanol. This enhances the turnover frequencies (TOF) of the oxygenates on the inverse catalysts. Therefore, the zirconia/copper interface could play a crucial molecular role in the CO_2 hydrogenation reaction, as it promotes the conversion of formate intermediates to methanol.

Hence, our primary objective in this section is to investigate the structures that contain formates adsorbed at the Cu-Zr interface, still under the more realistic catalytic condition (b). The bar graph in Figure 7 illustrates the fractions of structures that have formates adsorbed on the interface of Zr-Cu, which is very low. The formate adsorbs at the interface in a bidentate manner, with one oxygen atom interacting with Zr and the other interacting with the Cu surface. The four most favorable structures containing interface formates are (in increasing energy order) $Zr_3O_3(OH)_4(HCOO)_4$, $Zr_3O_3(OH)_4(HCOO)_4$, $Zr_3O_2(OH)_6(HCOO)_3$, $Zr_3O_3(OH)_5(HCOO)_3$ with the Boltzmann probability of 1.72%, 0.92%, 0.64%, and 0.34% respectively. The low content of formates, which could appear counterproductive to the reactivity, does not exclude the possibility of transient formates turning over to methanol. Indeed, some metastable structures containing interfacial formates (e.g., those show in Fig. 7) can be of low energy, only 0.1-0.2 eV above the GM. There are instances from our previous work where species with a probability of ~1% were

shown to be completely responsible for the catalytic reactivity[41,56–58]. All the structures identified in our study are highly hydroxylated. This is an encouraging observation as the hydrogen on the hydroxyl groups could potentially aid in the hydrogenation of formate to H_2COO at the interface between Zr and Cu.

E. Electronic structure analysis

Until this point, we considered the geometric structure of the active site, we will now focus in addition on its electronic structure and oxidation state. It is widely acknowledged that metallic copper and oxidized copper play crucial roles in the formation of methanol. Metallic copper facilitates the dissociative adsorption of hydrogen, which leads to the generation of atomic hydrogen. This atomic hydrogen on the surface participates in the hydrogenation of CO_2, either directly or indirectly by reforming the hydroxyl group. On the other hand, oxidized copper at the interface of Zr/Cu is considered as important for methanol formation, and its presence is essential for achieving high selectivity for methanol and low selectivity for CO under operating conditions.

Interestingly, it has been observed that metallic copper is more conducive to the RWGS reaction than partially oxidized copper, as previously documented in the literature[59]. The participation of Cu^+ species in the CO_2 hydrogenation to methanol has already been proposed, and researchers have explored this concept extensively. For instance, Klier et al. proposed that Cu^+ ions dissolved in the ZnO lattice serve as active sites for methanol synthesis from syngas and CO_2/H_2 mixtures on Cu/ZnO-based catalysts [60] .

Furthermore, Chinchen, Waugh et al. conducted a study using a series of $CO/CO_2/H_2$ mixtures over a commercial $Cu/ZnO/Al_2O_3$ catalyst. They discovered that the surface of the catalyst contained both metallic and oxidized copper under real methanol synthesis conditions, and the copper on the surface was more oxidized with a higher CO_2/CO ratio[53] . Similarly, Saito et al. reported comparable findings regarding methanol synthesis from CO_2/H_2, attributing the high performance of $Cu/ZnO/ZrO_2/Al_2O_3/Ga_2O_3$ to an optimal Cu^+/Cu ratio of approximately 0.7[61]. Homs et al. also observed the presence of Cu^+ states in the gallium-promoted ZnO-supported catalyst [62] .

The Cu cations act as Lewis acid centers by accepting electrons, while OH groups serve for further hydrogenation steps. These groups help to strengthen CO_2 adsorption and effectively activate the inert molecules. In summary, the interplay between metallic and oxidized copper plays a crucial role in the formation of methanol and involves complex chemical mechanisms that rely on the properties of copper species, including their oxidation state and associated acid-base characteristics.

In Figure 8, we investigate the impact of adsorbates on the Bader charges and on the possible oxidation of the Cu atoms. All Bader charges reported are referenced to the absolute charges for Zr(12) and Cu(11). Our analysis focuses on the Bader charges for the first layer of the Cu surface as well as the changes in Bader charges on the three Zr atoms. Panels (a) and (b) depict the global minimum structures with various x and y combinations with 2HCOO, while panels (c) and (d) represent the global minimum structures with various x and y combinations with 3HCOO. The white arrow indicates the change in the number of hydrogen atoms in the structure, with its direction representing an increase in the number of hydrogen atoms.

In panels (a) and (c), we observe the absolute Bader charge difference on the first layer of Cu, whereas panels (b) and (d) illustrate the absolute Bader charge difference on the Zr atoms. Notably, the addition or removal of hydrogen atoms does not cause any change in the charges on Zr (as observed in panels (b) and (d)), but it does affect the charges on the Cu surface (as seen in panels (a) and (c)). In this case, Cu acts as an "electron reservoir" adjusting to any changes in the electronic state caused by the addition or removal of the hydrogen atoms. On the other hand, alterations in the number of oxygen atoms impact both Zr and Cu charges. The changes in Zr charges are attributed to variations in the Zr coordination caused by the addition or subtraction of O in the cluster, which directly influences the electronic states of Zr. Conversely, the addition of hydrogen does not significantly alter the Zr cluster's coordination, as hydrogen interacts directly with oxygen to form protons on hydroxyl groups, keeping the overall coordination of Zr constant before and after the addition of H, while the electrons will migrate towards the metallic Cu surface. Similar to the case of O, formates do have an effect on the charges of both Zr and Cu as it again changes the coordinate states of Zr and also interact with Cu. The O and OH ligands first oxidize the Zr atoms, and if their number is sufficient for a complete oxidation of the three Zr,

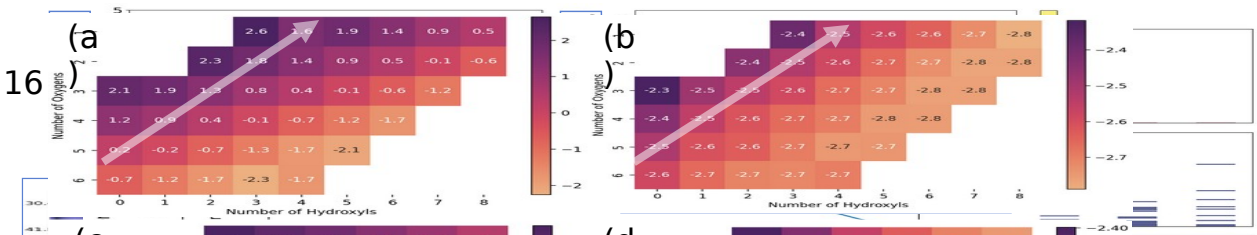

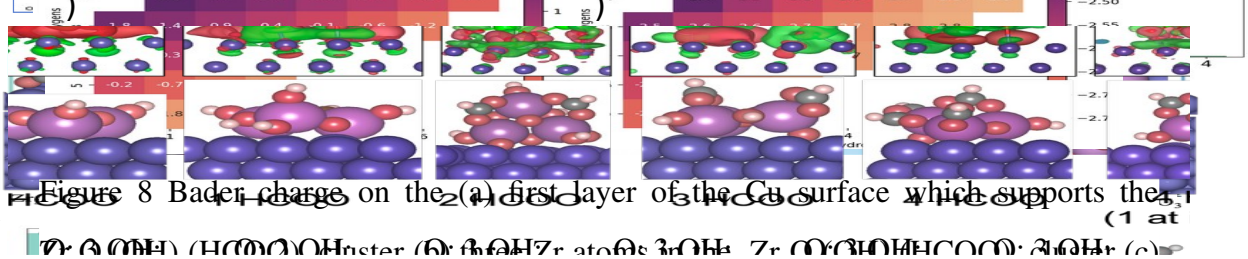

Figure 8 Bader charge on the (a) first layer of the Cu surface which supports the

Figure 9 : Charge density difference iso-surfaces along with the side view of different

structures. The green represents the negative iso-surface (charge depletion) whereas the red represents the positive iso-surface (charge accumulation). The number of Oxygen and Hydroxyls on the cluster are provided below the structures.

the number of hydroxyls on the cluster whereas the y axis is the number of oxygens on the cluster. The white arrow represents the change in the number of hydrogens on the cluster, with the number of hydrogens increasing in the direction of the arrow. The annotated value on the heat plot is the difference in the absolute Bader charges with more negative value meaning the atoms are oxidized (i.e. a decrease of the electronic population).

shown in (a) for the three different reaction conditions (top P=0.013 atm, middle P=4.93 atm and bottom P=30 atm).

cluster adsorption on the surface (Figure 9). The global minimum structure when no formate was present was $Zr_3O_3OH_3$/Cu. Upon calculating the oxidation state of the individual Zr in $Zr_3O_3OH_3$, it was determined to be Zr^{3+}, with one electron remaining in the valence. This electron remaining on Zr accumulates between the cluster and the Cu support, together with electronic density provided by Cu hence creating a bond between them. The electrons from the copper and Zr cluster are located precisely in between Cu and Zr (as seen in red for the 0HCOO case in Figure 9). As the concentration of formate increases, there is a notable alteration in the electron count. Specifically, as formate accumulates, Zr undergoes a change in its oxidation state, transitioning to Zr^{4+}. This shift results in a reduced availability of electrons for the binding of Zr atoms with Cu. Additionally, the presence of an increasing number of formate ligands significantly impacts the overall composition of the cluster, including the prevalence of oxygen (-O), hydroxyl (-OH), and formate (-HCOO) groups. For instance, as the formate concentration increases from 0 to 4, the amount of -O ligand can reach up to 4, and the -OH ligands can increase to as many as 7 hydroxyls, in the most favorable structures.

This surge in the concentration of ligands at the interface leads to substantial modifications in both the electronic structure and the relative positioning of Zr and Cu atoms. Consequently, Zr atoms tend to move farther away from Cu atoms, while hydroxyl and oxygen groups play a pivotal role in anchoring the Zr atoms to the Cu surface. In this context, at the interface, a combination of oxygen (-O) and hydroxyl (-OH) groups are present, and some Cu atoms undergo

oxidation. As a result of these changes, there is a depletion of charges at the interface, and the electronic distribution becomes predominantly centered around the oxygen and hydroxyl centers.

Our results directly concern the inverse catalyst, with ZrO_2 dispersed on a Cu support. Extension to the direct catalyst (Cu supported on ZrO_2) is delicate without further calculations. However, it can be expected that the Cu/ZrO_2 interface shows similarities between the two systems, and that at the interface of the direct catalyst (Cu on ZrO_2) significant amounts of -OH, -O and -HCOO will be present depending on the reaction conditions, with formate adsorbed either on the ZrO_2 support or at the interface of that support with Cu particles.

IV. CONCLUSION

In conclusion, our investigation into the inverse catalyst $Zr_3O_xOH_y(HCOO)_z$ /Cu(111) has highlighted that the catalyst cannot be described by a single structure, but that a large ensemble of structures can be present with rather equivalent probability, with different numbers of O, OH and formate ligands and varying interaction mode with the Cu(111) support. This fluxional nature of the catalysts sets a challenge for the study of the catalytic reactivity, since it requires to sample several active sites. In addition, we show a significant changes in this ensemble representation of active site upon modification of the reaction conditions, such as pressure, temperature, conversion, and CO_2:H_2 feed ratio. The evolution of the active site under particular reaction conditions is crucial for understanding the mechanism of CO_2 hydrogenation.

We found that, in reaction conditions, the free energy surface is relatively flat with respect to the number of hydroxyls and formates, suggesting that these groups play a vital role in facilitating the CO_2 hydrogenation reaction. The cluster can act as a reservoir for hydrogen, as the free energy surface does not change significantly with the gain or loss of hydrogens.

Oxygen and hydroxyl groups are primarily located on the Zr cations, with some bridging Zr and Cu, especially at high formate coverage. Formate species are adsorbed on the Zr-oxi-hydroxide moiety for all the most stable structures for the various conditions considered. However, we identified an ensemble of metastable structures with formates at the interface between Zr and Cu. It is expected that these metastable interfacial formates can have a specific role in the CO_2 hydrogenation to methanol and this will be the focus of future research. Our results in this study

have significant implications for the design of effective catalysts for CO_2 hydrogenation. By understanding the changes in the active site and the role of hydroxyls and formates, we can better engineer catalysts by choosing specific reaction conditions to promote this reaction. Our results show that care should be given when studying the catalyst in model conditions, such as low pressure, since different surface configurations occur under these circumstances.

Our investigation also revealed significant changes in the electronic state with the variation in oxygens, hydroxyls, and formates in the system. We observed partial oxidation of Cu as well as full oxidation of Zr. Literature has shown that Cu^+ may be crucial in the CO_2 hydrogenation reaction. Our findings on the electronic state changes highlight the need to consider the impact of reaction conditions on the catalyst's electronic structure. By recognizing the significance of certain electronic states, such as partial oxidation of Cu and full oxidation of Zr, we can tailor the catalyst's electronic properties to optimize its performance. This could guide the design of catalysts with optimal electronic properties, potentially leading to improved catalytic performance.

V. Conflicts of interest

There are no conflicts to declare.

VI. SUPPORTING INFORMATION AVAILABLE:

Full details on the Grand Canonical Basin Hopping algorithm. Full free energy surface heat plots for the reaction conditions (a) and (b) at different formate coverages.

VII. ACKNOWLEDGEMENTS

This work was supported by the grant DE-SC0019152 from the US Department of Energy, Office of Science, Basic Energy Science Program. This research used resources of the Innovative and Novel Computational Impact on Theory and Experiment (INCITE) program at the Argonne Leadership Computing Facility (theta machine, grant name ‘HetCatDynStates’), a U.S. Department of Energy Office of Science User Facility operated under Contract DE-AC02-06CH11357. This work used computational and storage services associated with the Hoffman2 Shared Cluster provided by the UCLA Institute for Digital Research and Education Research

Technology Group. This research used the resources of the National Energy Research Scientific Computing Center (NERSC), a U.S. Department of Energy Office of Science User Facility operated under Contract No. DE-AC02-05CH11231. The authors want to thank XSEDE SDSC's Comet, Expanse Supercomputer, and Bridges PSC for the computation time.

VIII. REFERENCES:

(1) Graciani, J.; Mudiyanselage, K.; Xu, F.; Baber, A. E.; Evans, J.; Senanayake, S. D.; Stacchiola, D. J.; Liu, P.; Hrbek, J.; Fernández Sanz, J.; Rodriguez, J. A. Catalysis. Highly Active Copper-Ceria and Copper-Ceria-Titania Catalysts for Methanol Synthesis from CO_2. *Science* **2014**, *345* (6196), 546–550. https://doi.org/10.1126/SCIENCE.1253057.

(2) Centi, G.; Quadrelli, E. A.; Perathoner, S. Catalysis for CO2 Conversion: A Key Technology for Rapid Introduction of Renewable Energy in the Value Chain of Chemical Industries. *Energy Environ Sci* **2013**, *6* (6), 1711–1731. https://doi.org/10.1039/C3EE00056G.

(3) Dorner, R. W.; Hardy, D. R.; Williams, F. W.; Willauer, H. D. Heterogeneous Catalytic CO 2 Conversion to Value-Added Hydrocarbons. *Energy Environ Sci* **2010**, *3* (7), 884–890. https://doi.org/10.1039/C001514H.

(4) Inui, T.; Takeguchi, T. Effective Conversion of Carbon Dioxide and Hydrogen to Hydrocarbons. *Catal Today* **1991**, *10* (1), 95–106. https://doi.org/10.1016/0920-5861(91)80077-M.

(5) Kondratenko, E. V.; Mul, G.; Baltrusaitis, J.; Larrazábal, G. O.; Pérez-Ramírez, J. Status and Perspectives of CO2 Conversion into Fuels and Chemicals by Catalytic, Photocatalytic and Electrocatalytic Processes. *Energy Environ Sci* **2013**, *6* (11), 3112–3135. https://doi.org/10.1039/C3EE41272E.

(6) Behrens, M.; Studt, F.; Kasatkin, I.; Kühl, S.; Hävecker, M.; Abild-Pedersen, F.; Zander, S.; Girgsdies, F.; Kurr, P.; Kniep, B. L.; Tovar, M.; Fischer, R. W.; Nørskov, J. K.; Schlögl, R. The Active Site of Methanol Synthesis over Cu/ZnO/ Al2O3 Industrial Catalysts. *Science* **2012**, *336* (6083), 893–897. https://doi.org/10.1126/SCIENCE.1219831.

(7) Nie, X.; Esopi, M. R.; Janik, M. J.; Asthagiri, A. Selectivity of CO2 Reduction on Copper Electrodes: The Role of the Kinetics of Elementary Steps. *Angewandte Chemie - International Edition* **2013**, *52* (9), 2459–2462. https:// doi.org/10.1002/ANIE.201208320.

(8) Yang, H.; Xu, Z.; Fan, M.; Gupta, R.; Slimane, R. B.; Bland, A. E.; Wright, I. Progress in Carbon Dioxide Separation and Capture: A Review. *Journal of Environmental Sciences* **2008**, *20* (1), 14–27. https://doi.org/10.1016/S1001-0742(08)60002-9.

(9) Aresta, M.; Dibenedetto, A.; Angelini, A. Catalysis for the Valorization of Exhaust Carbon: From CO2 to Chemicals, Materials, and Fuels. Technological Use of CO2. *Chem Rev* **2014**, *114* (3), 1709–1742. https://doi.org/10.1021/CR4002758.

(10) Studt, F.; Sharafutdinov, I.; Abild-Pedersen, F.; Elkjær, C. F.; Hummelshøj, J. S.; Dahl, S.; Chorkendorff, I.; Nørskov, J. K. Discovery of a Ni-Ga Catalyst for Carbon Dioxide Reduction to Methanol. *Nat Chem* **2014**, *6* (4), 320–324. https://doi.org/10.1038/NCHEM.1873.
(11) Porosoff, M. D.; Yan, B.; Chen, J. G. Catalytic Reduction of CO2 by H2 for Synthesis of CO, Methanol and Hydrocarbons: Challenges and Opportunities. *Energy Environ Sci* **2016**, *9* (1), 62–73. https://doi.org/10.1039/C5EE02657A.
(12) Morales-Guio, C.; Shen, K.; Yu-Chao, H.; Jang, J. Electrochemical Oxidation of Methane to Methanol on Electrodeposited Transition Metal Oxides. **2022**. https://doi.org/10.29363/NANOGE.NFM.2022.212.
(13) Shen, K.; Kumari, S.; Huang, Y.-C.; Jang, J.; Sautet, P.; Morales-Guio, C. G. Electrochemical Oxidation of Methane to Methanol on Electrodeposited Transition Metal Oxides. *J Am Chem Soc* **2023**, *145* (12), 6927–6943. https://doi.org/10.1021/jacs.3c00441.
(14) Wang, Y.; Kattel, S.; Gao, W.; Li, K.; Liu, P.; Chen, J. G.; Wang, H. Exploring the Ternary Interactions in Cu–ZnO–ZrO 2 Catalysts for Efficient CO 2 Hydrogenation to Methanol. *Nat Commun* **2019**, *10* (1). https://doi.org/10.1038/S41467-019-09072-6.
(15) Rungtaweevoranit, B.; Baek, J.; Araujo, J. R.; Archanjo, B. S.; Choi, K. M.; Yaghi, O. M.; Somorjai, G. A. Copper Nanocrystals Encapsulated in Zr-Based Metal-Organic Frameworks for Highly Selective CO2 Hydrogenation to Methanol. *Nano Lett* **2016**, *16* (12), 7645–7649. https://doi.org/10.1021/ACS.NANOLETT.6B03637/ASSET/IMAGES/LARGE/NL-2016-03637E_0004.JPEG.
(16) Studt, F.; Behrens, M.; Kunkes, E. L.; Thomas, N.; Zander, S.; Tarasov, A.; Schumann, J.; Frei, E.; Varley, J. B.; Abild-Pedersen, F.; Nørskov, J. K.; Schlögl, R. The Mechanism of CO and CO2 Hydrogenation to Methanol over Cu-Based Catalysts. *ChemCatChem* **2015**, *7* (7), 1105–1111. https://doi.org/10.1002/CCTC.201500123.
(17) Waugh, K. C. Methanol Synthesis. *Catal Today* **1992**, *15* (1), 51–75. https://doi.org/10.1016/0920-5861(92)80122-4.
(18) Liu, X. M.; Lu, G. Q.; Yan, Z. F.; Beltramini, J. Recent Advances in Catalysts for Methanol Synthesis via Hydrogenation of CO and CO2. *Ind Eng Chem Res* **2003**, *42* (25), 6518–6530. https://doi.org/10.1021/IE020979S/ASSET/IMAGES/MEDIUM/IE020979SE00022.GIF.
(19) Yang, Y.; Evans, J.; Rodriguez, J. A.; White, M. G.; Liu, P. Fundamental Studies of Methanol Synthesis from CO2 Hydrogenation on Cu(111), Cu Clusters, and Cu/ZnO(000). *Physical Chemistry Chemical Physics* **2010**, *12* (33), 9909–9917. https://doi.org/10.1039/C001484B.
(20) Yang, Y.; White, M. G.; Liu, P. Theoretical Study of Methanol Synthesis from CO 2 Hydrogenation on Metal-Doped Cu(111) Surfaces. *Journal of Physical Chemistry C* **2012**, *116* (1), 248–256. https://doi.org/10.1021/JP208448C/ASSET/IMAGES/LARGE/JP-2011-08448C_0004.JPEG.

(21) Rui, N.; Shi, R.; Gutiérrez, R. A.; Rosales, R.; Kang, J.; Mahapatra, M.; Ramírez, P. J.; Senanayake, S. D.; Rodriguez, J. A. CO2 Hydrogenation on ZrO2/Cu(111) Surfaces: Production of Methane and Methanol. *Ind Eng Chem Res* **2021**. https://doi.org/10.1021/ACS.IECR.1C03229.
(22) Tada, S.; Kayamori, S.; Honma, T.; Kamei, H.; Nariyuki, A.; Kon, K.; Toyao, T.; Shimizu, K. I.; Satokawa, S. Design of Interfacial Sites between Cu and Amorphous ZrO2 Dedicated to CO2-to-Methanol Hydrogenation. *ACS Catal* **2018**, *8* (9), 7809–7819. https://doi.org/10.1021/ACSCATAL.8B01396.
(23) Witoon, T.; Chalorngtham, J.; Dumrongbunditkul, P.; Chareonpanich, M.; Limtrakul, J. CO2 Hydrogenation to Methanol over Cu/ZrO2 Catalysts: Effects of Zirconia Phases. *Chemical Engineering Journal* **2016**, *293*, 327–336. https://doi.org/10.1016/J.CEJ.2016.02.069.
(24) Witoon, T.; Chalorngtham, J.; Dumrongbunditkul, P.; Chareonpanich, M.; Limtrakul, J. CO2 Hydrogenation to Methanol over Cu/ZrO2 Catalysts: Effects of Zirconia Phases. *Chem. Eng. J.* **2016**, *293*, 327–336. https://doi.org/10.1016/j.cej.2016.02.069.
(25) Reichenbach, T.; Mondal, K.; Jäger, M.; Vent-Schmidt, T.; Himmel, D.; Dybbert, V.; Bruix, A.; Krossing, I.; Walter, M.; Moseler, M. Ab Initio Study of CO2 Hydrogenation Mechanisms on Inverse ZnO/Cu Catalysts. *J Catal* **2018**, *360*, 168–174. https://doi.org/10.1016/J.JCAT.2018.01.035.
(26) Wu, C.; Lin, L.; Liu, J.; Zhang, J.; Zhang, F.; Zhou, T.; Rui, N.; Yao, S.; Deng, Y.; Yang, F.; Xu, W.; Luo, J.; Zhao, Y.; Yan, B.; Wen, X. D.; Rodriguez, J. A.; Ma, D. Inverse ZrO2/Cu as a Highly Efficient Methanol Synthesis Catalyst from CO2 Hydrogenation. *Nat Commun* **2020**, *11* (1). https://doi.org/10.1038/S41467-020-19634-8.
(27) Hong, Q. J.; Liu, Z. P. Mechanism of CO2 Hydrogenation over Cu/ZrO2($\bar{2}$12) Interface from First-Principles Kinetics Monte Carlo Simulations. *Surf Sci* **2010**, *604* (21–22), 1869–1876. https://doi.org/10.1016/J.SUSC.2010.07.018.
(28) Zhuang, H. D.; Bai, S. F.; Liu, X. M.; Yan, Z. F. Structure and Performance of Cu/ZrO2 Catalyst For the Synthesis of Methanol from CO2 Hydrogenation. *Journal of Fuel Chemistry and Technology* **2010**, *38* (4), 462–467. https://doi.org/10.1016/S1872-5813(10)60041-2.
(29) Zhao, H.; Yu, R.; Ma, S.; Xu, K.; Chen, Y.; Jiang, K.; Fang, Y.; Zhu, C.; Liu, X.; Tang, Y.; Wu, L.; Wu, Y.; Jiang, Q.; He, P.; Liu, Z.; Tan, L. The Role of Cu1–O3 Species in Single-Atom Cu/ZrO2 Catalyst for CO2 Hydrogenation. *Nature Catalysis 2022 5:9* **2022**, *5* (9), 818–831. https://doi.org/10.1038/s41929-022-00840-0.
(30) Wang, Y.; Kattel, S.; Gao, W.; Li, K.; Liu, P.; Chen, J. G.; Wang, H. Exploring the Ternary Interactions in Cu-ZnO-ZrO2 Catalysts for Efficient CO2 Hydrogenation to Methanol. *Nat. Commun.* **2019**, *10* (1). https://doi.org/10.1038/s41467-019-09072-6.
(31) Wang, J.; Li, G.; Li, Z.; Tang, C.; Feng, Z.; An, H.; Liu, H.; Liu, T.; Li, C. A Highly Selective and Stable ZnO-ZrO2 Solid Solution Catalyst for CO2 Hydrogenation to Methanol. *Sci. Adv.* **2017**, *3* (10), e1701290. https://doi.org/10.1126/sciadv.1701290.

(32) Guo, X.; Mao, D.; Lu, G.; Wang, S.; Wu, G. Glycine-Nitrate Combustion Synthesis of CuO-ZnO-ZrO2 Catalysts for Methanol Synthesis from CO2 Hydrogenation. *J Catal* **2010**, *271* (2), 178–185. https://doi.org/10.1016/J.JCAT.2010.01.009.
(33) Samson, K.; Sliwa, M.; Socha, R. P.; Góra-Marek, K.; Mucha, D.; Rutkowska-Zbik, D.; Paul, J. F.; Ruggiero-Mikoajczyk, M.; Grabowski, R.; Soczyński, J. Influence of ZrO2 Structure and Copper Electronic State on Activity of Cu/ZrO2 Catalysts in Methanol Synthesis from CO2. *ACS Catal* **2014**, *4* (10), 3730–3741. https://doi.org/10.1021/CS500979C/SUPPL_FILE/CS500979C_SI_002.PDF.
(34) Kattel, S.; Yan, B.; Yang, Y.; Chen, J. G.; Liu, P. Optimizing Binding Energies of Key Intermediates for CO2 Hydrogenation to Methanol over Oxide-Supported Copper. *J Am Chem Soc* **2016**, *138* (38), 12440–12450. https://doi.org/10.1021/JACS.6B05791.
(35) Li, K.; Chen, J. G. CO2 Hydrogenation to Methanol over ZrO2-Containing Catalysts: Insights into ZrO2 Induced Synergy. *ACS Catal* **2019**, *9* (9), 7840–7861. https://doi.org/10.1021/ACSCATAL.9B01943.
(36) Denise, B.; Cherifi, O.; Bettahar, M. M.; Sneeden, R. P. A. Supported Copper Catalysts Prepared from Copper(II) Formate. Hydrogenation of Carbon Dioxide Containing Feedstocks. *Appl Catal* **1989**, *48* (2). https://doi.org/10.1016/S0166-9834(00)82805-5.
(37) Nitta, Y.; Suwata, O.; Ikeda, Y.; Okamoto, Y.; Imanaka, T. Copper-Zirconia Catalysts for Methanol Synthesis from Carbon Dioxide: Effect of ZnO Addition to Cu-ZrO2 Catalysts. *Catal Letters* **1994**, *26* (3–4). https://doi.org/10.1007/BF00810608.
(38) Larmier, K.; Liao, W. C.; Tada, S.; Lam, E.; Verel, R.; Bansode, A.; Urakawa, A.; Comas-Vives, A.; Copéret, C. CO2-to-Methanol Hydrogenation on Zirconia-Supported Copper Nanoparticles: Reaction Intermediates and the Role of the Metal–Support Interface. *Angewandte Chemie International Edition* **2017**, *56* (9), 2318–2323. https://doi.org/10.1002/ANIE.201610166.
(39) Ma, Y.; Wang, J.; Goodman, K. R.; Head, A. R.; Tong, X.; Stacchiola, D. J.; White, M. G. Reactivity of a Zirconia−Copper Inverse Catalyst for CO 2 Hydrogenation. *J. Phys. Chem. C* **2020**, *124*. https://doi.org/10.1021/acs.jpcc.0c06624.
(40) Kumari, S.; Sautet, P. Elucidation of the Active Site for the Oxygen Evolution Reaction on a Single Pt Atom Supported on Indium Tin Oxide. *Journal of Physical Chemistry Letters* **2023**, 2635–2643. https://doi.org/10.1021/ACS.JPCLETT.3C00160.
(41) Kumari, S.; Masubuchi, T.; White, H. S.; Alexandrova, A.; Anderson, S. L.; Sautet, P. Electrocatalytic Hydrogen Evolution at Full Atomic Utilization over ITO-Supported Sub-Nano-Ptn Clusters: High, Size-Dependent Activity Controlled by Fluxional Pt Hydride Species. *J Am Chem Soc* **2023**. https://doi.org/10.1021/JACS.2C13063.
(42) Zhai, H.; Alexandrova, A. N. Fluxionality of Catalytic Clusters: When It Matters and How to Address It. *ACS Catal* **2017**, *7* (3), 1905–1911.

https://doi.org/10.1021/ACSCATAL.6B03243/ASSET/IMAGES/LARGE/CS-2016-03243J_0009.JPEG.
(43) Sun, G.; Alexandrova, A. N.; Sautet, P. Structural Rearrangements of Subnanometer Cu Oxide Clusters Govern Catalytic Oxidation. *ACS Catal* **2020**, *10* (9), 5309–5317. https://doi.org/10.1021/ACSCATAL.0C00824/SUPPL_FILE/CS0C00824_SI_002.PDF.
(44) Sun, G.; Alexandrova, A. N.; Sautet, P. Pt8 Cluster on Alumina under a Pressure of Hydrogen: Support-Dependent Reconstruction from First-Principles Global Optimization. *J Chem Phys* **2019**, *151* (19), 194703. https://doi.org/10.1063/1.5129296.
(45) Zhang, Z.; Masubuchi, T.; Sautet, P.; Anderson, S. L.; Alexandrova, A. N.; Zhang, Z.; Sautet, P.; Alexandrova, A. N.; Masubuchi, T.; Anderson, S. L. Hydrogen Evolution on FTO-Supported Ptn Clusters: Ensemble of Hydride States Governs the Size Dependent Reactivity. **2022**. https://doi.org/10.26434/CHEMRXIV-2022-SSH9N.
(46) Kumari, S.; Sautet, P. Highly Dispersed Pt Atoms and Clusters on Hydroxylated Indium Tin Oxide: A View from First-Principles Calculations. *J. Mater. Chem. A* **2021**, *9*, 15724.
(47) Kresse, G.; Furthmüller, J. Efficient Iterative Schemes for Ab Initio Total-Energy Calculations Using a Plane-Wave Basis Set. *Phys Rev B Condens Matter Mater Phys* **1996**, *54* (16), 11169–11186. https://doi.org/10.1103/PhysRevB.54.11169.
(48) Kresse, G. Ab Initio Molecular Dynamics for Liquid Metals. *J Non Cryst Solids* **1995**, *192–193*, 222–229. https://doi.org/10.1016/0022-3093(95)00355-X.
(49) Blöchl, P. E. Projector Augmented-Wave Method. *Phys Rev B* **1994**, *50* (24), 17953–17979. https://doi.org/10.1103/PhysRevB.50.17953.
(50) Perdew, J. P.; Burke, K.; Ernzerhof, M. Generalized Gradient Approximation Made Simple. *Phys Rev Lett* **1996**, *77* (18), 3865–3868. https://doi.org/10.1103/PhysRevLett.77.3865.
(51) Liu, L.; Su, X.; Zhang, H.; Gao, N.; Xue, F.; Ma, Y.; Jiang, Z.; Fang, T. Zirconia-Modified Copper Catalyst for CO2 Conversion to Methanol from DFT Study. *Appl Surf Sci* **2020**, *528*, 146900. https://doi.org/10.1016/J.APSUSC.2020.146900.
(52) Tang, X.; Zhang, H.; Sun, C.; Qiao, X.; Ju, D. Adsorption Mechanisms over ZrO2-Modified Cu(1 1 1) Surface for X (CH3OH, H2O and CO): A DFT+U Study. *Surf Sci* **2022**, *716*, 121976. https://doi.org/10.1016/J.SUSC.2021.121976.
(53) Chinchen, G. C.; Denny, P. J.; Parker, D. G.; Spencer, M. S.; Whan, D. A. Mechanism of Methanol Synthesis from CO2/CO/H2 Mixtures over Copper/Zinc Oxide/Alumina Catalysts: Use Of14C-Labelled Reactants. *Appl Catal* **1987**, *30* (2), 333–338. https://doi.org/10.1016/S0166-9834(00)84123-8.
(54) Ha, M. A.; Dadras, J.; Alexandrova, A. Rutile-Deposited Pt-Pd Clusters: A Hypothesis Regarding the Stability at 50/50 Ratio. *ACS Catal* **2014**, *4* (10), 3570–3580. https://doi.org/10.1021/CS5011426.

(55) Meng, G.; Arkus, N.; Brenner, M. P.; Manoharan, V. N. The Free-Energy Landscape of Clusters of Attractive Hard Spheres. *Science (1979)* **2010**, *327* (5965), 560–563. https://doi.org/10.1126/SCIENCE.1181263/SUPPL_FILE/MENG.SOM.PDF.
(56) Sun, G.; Sautet, P. Metastable Structures in Cluster Catalysis from First-Principles: Structural Ensemble in Reaction Conditions and Metastability Triggered Reactivity. *J Am Chem Soc* **2018**, *140* (8), 2812–2820. https://doi.org/10.1021/JACS.7B11239/ASSET/IMAGES/JA-2017-11239P_M008.GIF.
(57) Zhang, Z.; Cui, Z. H.; Jimenez-Izal, E.; Sautet, P.; Alexandrova, A. N. Hydrogen Evolution on Restructured B-Rich WB: Metastable Surface States and Isolated Active Sites. *ACS Catal* **2020**, *10* (23), 13867–13877. https://doi.org/10.1021/acscatal.0c03410.
(58) Poths, P.; Li, G.; Masubuchi, T.; Morgan, H. W. T.; Zhang, Z.; Alexandrova, A. N.; Anderson, S. L. Got Coke? Self-Limiting Poisoning Makes an Ultra Stable and Selective Sub-Nano Cluster Catalyst. *ACS Catal* **2023**, *13* (2), 1533–1544. https://doi.org/10.1021/ACSCATAL.2C05634/SUPPL_FILE/CS2C05634_SI_001.PDF.
(59) Campbell, C. T.; Ernst, K.-H. Forward and Reverse Water—Gas Shift Reactions on Model Copper Catalysts. **1992**, 130–142. https://doi.org/10.1021/BK-1992-0482.CH008.
(60) Klier, K. Methanol Synthesis. *Advances in Catalysis* **1982**, *31* (C), 243–313. https://doi.org/10.1016/S0360-0564(08)60455-1.
(61) Saito, M.; Fujitani, T.; Takeuchi, M.; Watanabe, T. Development of Copper/Zinc Oxide-Based Multicomponent Catalysts for Methanol Synthesis from Carbon Dioxide and Hydrogen. *Appl Catal A Gen* **1996**, *138* (2), 311–318. https://doi.org/10.1016/0926-860X(95)00305-3.
(62) Toyir, J.; De la Piscina, P. R.; Fierro, J. L. G.; Homs, N. Catalytic Performance for CO2 Conversion to Methanol of Gallium-Promoted Copper-Based Catalysts: Influence of Metallic Precursors. *Appl Catal B* **2001**, *34* (4), 255–266. https://doi.org/10.1016/S0926-3373(01)00203-X.

TABLE OF CONTENTS ARTWORK